ASTRONOMY & ASTROPHYSICS
SUPPLEMENT SERIES

Astron. Astrophys. Suppl. Ser. **147**, 99–109 (2000)

CCD photometric search for peculiar stars in open clusters

I. NGC 2169, Melotte 105 and NGC 6250⋆

C. Bayer[1], **H.M. Maitzen**[1], **E. Paunzen**[1,2], **M. Rode-Paunzen**[1], **and M. Sperl**[1]

[1] Institut für Astronomie der Universität Wien, Türkenschanzstr. 17, A-1180 Wien, Austria
[2] Zentraler Informatikdienst der Universität Wien, Universitätsstr. 7, A-1010 Wien, Austria

Received April 3; accepted August 25, 2000

Abstract. The search for chemically peculiar (CP) stars in open clusters using photoelectric photometry sampling the presence of the characteristic flux depression feature at 5200 Å via the Δa-system (Maitzen 1976) has so far delivered data for objects usually no more distant than 1000 pc from the Sun. A series of fourteen papers (first: Maitzen & Hensberge 1981; for the time being last: Maitzen 1993) were devoted to 1240 stars in 38 open cluster fields.

If one intends to study the presence of CP stars at larger distances from the Sun, classical photometry has to be replaced by CCD photometry. We have therefore initialized in 1995 a new survey in open clusters and the Large Magellanic Cloud using the CCD technology.

As a first step, we have presented new Δa-photometry of 22 CP2 stars in the galactic field to prove the capability of CCD photometry for our aim (Maitzen et al. 1997).

In the first paper of a new series devoted to CCD photometry, we present data on NGC 2169 (13 stars investigated), Melotte 105 (114 stars), and NGC 6250 (48 stars). NGC 2169 was used to test our results with those of classical photometry which yields excellent agreement.

For NGC 6250 we find two new definite CP2 (according to the definition by Preston 1974) stars ($\Delta a = 0.065$ and 0.026 mag) and two λ Bootis candidates. Twelve objects with only marginally peculiar Δa-values for Melotte 105 were detected. Additional spectroscopic and photometric evidence is needed to substantiate their peculiarity.

Key words: stars: chemically peculiar — stars: early-type — techniques: photometric — open clusters and associations: general

Send offprint requests to: E. Paunzen,
e-mail: Ernst.Paunzen@univie.ac.at

⋆ Based on observations at ESO-La Silla, UTSO-Las Campanas and L. Figl Observatory, Mt. Schöpfl, Austria.

1. Introduction

In a serie of papers (first: Maitzen & Hensberge 1981; for the time being last: Maitzen 1993) 38 open clusters have been surveyed for the presence of magnetic peculiar stars using Δa-photometry in the conventional photomultiplier technique. The advantage of this approach is both a relatively high accuracy of the detection index Δa (external scatter for normal stars 0.003 to 0.005 mag) and its immediate availability, hence detection of CP2 stars at the telescope. Using photoelectric photometry, on the other hand, the magnitude limit is about $V = 12$ mag for work with a 1 m telescope. This limit corresponds to a vicinity of only about 1000 pc around the Sun. Even in this area we can reach only the hotter sections of CP2 stars depending on the amount of interstellar absorption.

If one aims to study the behaviour and appearance of peculiar stars over a significant range of galactocentric distances – speculating about the possible influence of different degrees of metallicity and/or galactic magnetic field strengths – then it is imperative to increase the actual magnitude limit by at least two or three magnitudes. Discarding the availability of 4 m telescopes as highly unrealistic we are left with employing the CCD-technique. Maitzen et al. (1997) have prepared the ground by showing that for field stars in the range $8 < V < 10$ mag Δa-values obtained with CCD-photometry at a 60 cm telescope exhibit essentially the same error level as conventional photoelectric photometry.

Aside from the basic advantage of CCD-photometry – i.e. simultaneous recording of many individual objects not only saving time but also increasing precision – the second benefit becomes more and more obvious when observing clusters at larger distances with decreasing angular separations of their members. In this case stellar magnitudes can be derived only by fitting of individual point-spread-functions.

Table 1. Observation log

Cluster	Site	Nights	$\#_{g_1}$	$\#_{g_2}$	$\#_y$
NGC 2169	L. Figl Obs.	1	5	3	3
Melotte 105	ESO	4	9	12	10
NGC 6250	ESO	6	19	20	19
	UTSO	1	2	2	2

Table 2. Characteristics of the used filters

Filter	λ_C [Å]	Bandwidth [Å]	Transmission [%]
g_1	5027	222	66
g_2	5205	107	50
y	5509	120	54

This paper presents the first three open clusters, NGC 2169, Melotte 105 and NGC 6250 measured in the Δa system.

2. The Δa photometric system

Since this is the first paper of a new series about the Δa photometric system, we will give a short introduction to its basic properties and characteristics. The photometric system itself was defined by Maitzen (1976). It measures the broad band absorption feature at 5200 Å sampling the depth of this flux depression by comparing the flux at the center (5220 Å, g_2), with the adjacent regions (5000 Å, g_1 and 5500 Å, y). The respective index was introduced as:

$a = g_2 - (g_1 + y)/2.$

Since this quantity is slightly dependent on temperature (increasing towards lower temperatures), the intrinsic peculiarity index had to be defined as

$\Delta a = a - a_0[(b-y); (B-V); (g_1-y)]$

i.e. the difference between the individual a-value and the a-value of non-peculiar stars of the same colour (the locus of the a_0-values has been called normality line). It was shown (e.g. Vogt et al. 1998) that virtually all peculiar stars with magnetic fields (CP2 stars) have positive Δa-values up to 0.075 mag whereas Be and λ Bootis stars exhibit significant negative ones. Note that $(g_1 - y)$ shows an excellent correlation with $(b - y)$ and can be used as an index for the effective temperature.

As diagnostic tool the a versus $(g_1 - y)$ diagram is used. Assuming that all stars exhibit the same interstellar reddening, peculiar objects deviate from the normality line more than 3σ. Since most of the the clusters are reddened, their normality line is shifted by $E(b-y)$ to the red and by a small amount $E(a)$ to higher a-values (Maitzen 1993). The ratio of these shifts

$f = E(a)/E(b-y)$

can be determined from the deviation of a reddened cluster normality line from the unreddened relationship.

Table 3. Summary of results

Name	NGC 2169	Melotte 105	NGC 6250
Name	C0605+139	C1117−632	C1654−457
l/b	195/−3	293/−3	341/−2
$E(B-V)$	0.12	0.36	0.38
d [pc]	1100	2100	1020
$\log t$	7.70	7.77	7.15
Tr-type	III 3 m	I 2 p	II 3 r
n(obj)	13	114	48
n(members)	11	107	35
Δa/obj	+0.042/#12	−0.019/#6	+0.026/#8
		−0.022/#33	−0.027/#28
		−0.017/#38	−0.033/#45
		+0.015/#46	+0.065/#46
		+0.015/#66	
		−0.033/#70	
		−0.039/#75	
		+0.019/#76	
		+0.017/#78	
		−0.025/#107	
		−0.017/#112	
		−0.016/#113	

On the other hand, assuming a mean f-value (≈ 0.05) and iterating the formula

$a(\mathrm{corr}) = a(\mathrm{obs}) - fE(b-y)$

one can determine reddening values by the Δa photometry of clusters. More of a problem is the estimation of differential reddening within a cluster. In principle, two methods have been applied to overcome this problem:

- to deredden each individual object using the Strömgren $uvby\beta$ photometric system and its calibrations;
- to use the Q-method for the Johnson UBV photometric system.

An a versus $(b-y)_0$ or $(B-V)_0$ diagram should then be able to sort out the true peculiar objects.

3. Observations and reduction

Observations were performed with the Bochum 61 cm (ESO-La Silla) as well as the Helen-Sawyer-Hogg 61 cm telescope (UTSO-Las Campanas Observatory) during a campaign in April/May 1995 during which roughly three dozens of open clusters were observed. For comparison we also present results on NGC 2169 observed at the L. Figl Observatory with the 150 cm telescope on Mt. Schöpfl (Austria) using the multimode instrument OEFOSC. The detailed observation log is listed in Table 1.

The Bochum Telescope was equipped with a nitrogen-cooled Thompson 7882 CCD with 384 × 576 pixel, corresponding to a field-of-view of about $3' \times 4'$,

Table 4. All observed stars for NGC 2169

No.	V	$(b-y)$	a	(g_1-y)	Δa	$\Delta a_{\rm M93}$
4	8.61	0.024	0.602	−0.722	−0.003	+0.007
5	8.78	0.054	0.616	−0.698	+0.006	+0.003
6	9.13	0.073	0.617	−0.683	+0.004	+0.000
11	10.57	0.084	0.616	−0.674	+0.002	+0.002
12	10.79	0.071	0.657	−0.685	+0.044	+0.042
13	10.79	0.085	0.610	−0.673	−0.005	−0.003
14	10.87	0.131	0.626	−0.637	+0.003	+0.002
15	11.06	0.130	0.630	−0.637	+0.008	−0.010
16	11.18	0.124	0.620	−0.642	−0.001	−0.002
18	11.78	0.115	0.609	−0.649	−0.011	−0.005

Column 1: Notation according to Hoag et al. (1961).
Column 2: Visual magnitude from Hoag et al. (1961).
Column 3: $(b-y)$ from Perry et al. (1978).
Column 4: Mean a-index.
Column 5: Mean (g_1-y) value.
Column 6: Deviation from cluster line $a_0 = 0.767 + 0.227\,(g_1-y)$.
Column 7: Δa-value from Maitzen (1993).

the Helen-Sawyer-Hogg telescope with a water-cooled PM512 (516 × 516 pixel) equivalent to $4' \times 4'$ and the OEFOSC with a 512 × 512 pixel CCD corresponding to $5.5' \times 5.5'$ on the sky. The characteristics of the filters used are listed in Table 2.

The basic reductions (bias-subtraction, dark-correction, flat-fielding) were carried out within standard IRAF routines. For Melotte 105 we have applied a point-spread-function-fitting within the IRAF task DAOPHOT. For NGC 2169 and NGC 6250 standard aperture photometry within the IRAF task APPHOT was carried out due to the wide separation of the cluster members. Because of an instrumentally induced offsets between the single frames, photometry of each frame was performed separately and the measurements were then averaged. Due to the rather large area covered by NGC 6250, 64 frames, in total, were taken in two different fields – nine to twelve frames for each filter and center (note that the two different areas do not overlap).

4. Discussion

A summary of the results for the three investigated clusters is listed in Table 3 (based in part on Lyngå 1987). The pertinent numerical results for the individual clusters are given in the subsequent Tables 4, 5 and 6. The Δa-photometry of the three clusters is displayed in Figs. 1, 3 and 6. Candidate peculiar stars in all three clusters were selected if their mean Δa-values are 3σ outside the corresponding confidence intervals.

In the following we discuss special features of the individual clusters.

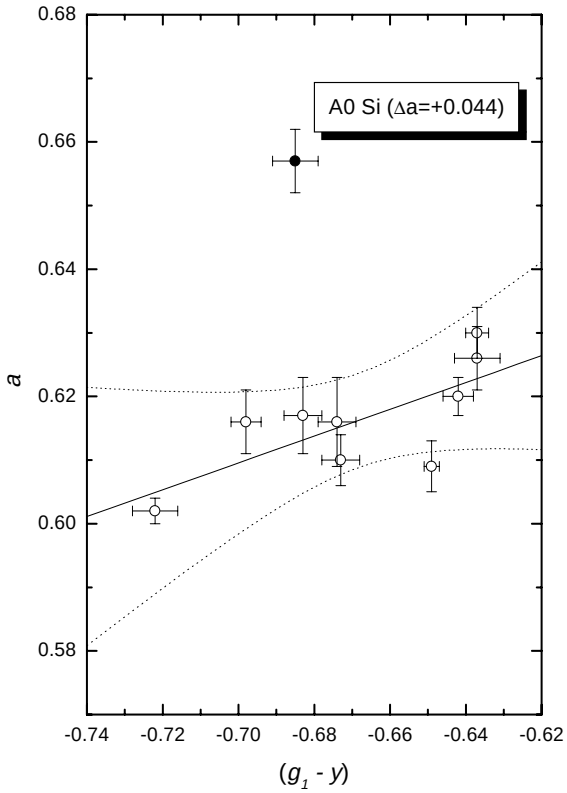

Fig. 1. a versus (g_1-y) for NGC 2169, indicated is the location of the well known A0 Si star. Filled circles indicate apparent peculiar stars whereas open circles are non-peculiar objects. The full line is the normality line whereas the dotted lines are the confidence intervals corresponding to 99.9 percent. The error bars for each individual objects are the mean errors

4.1. NGC 2169

This cluster in Orion was observed in order to test our results with previously published ones. Maitzen (1993) listed photoelectric observations of 15 stars with one prominent CP2 star (No. 12). We reobserved 10 stars of his list (note that our field-of-view was not large enough to cover the whole cluster) and find an excellent agreement with his values. Although we had only 11 frames in total, the scatter is remarkably small (0.0032 mag). The main reason is the brightness of the cluster members and the resulting good photon statistics. The stars observed in Melotte 105, for instance, are on the average four magnitudes fainter than those of NGC 2169.

Table 4 gives our results compared to those of Maitzen (1993). The A0 Si star No. 12 was listed in Maitzen (1993) with $\Delta a = +0.042$ mag whereas we find $\Delta a = +0.044$ mag.

The normality lines based on $(b-y)$ and (g_1-y), respectively, are given as:

$$a_0 = 0.601 + 0.164\,(b-y)$$

and

$$a_0 = 0.767 + 0.227\,(g_1-y).$$

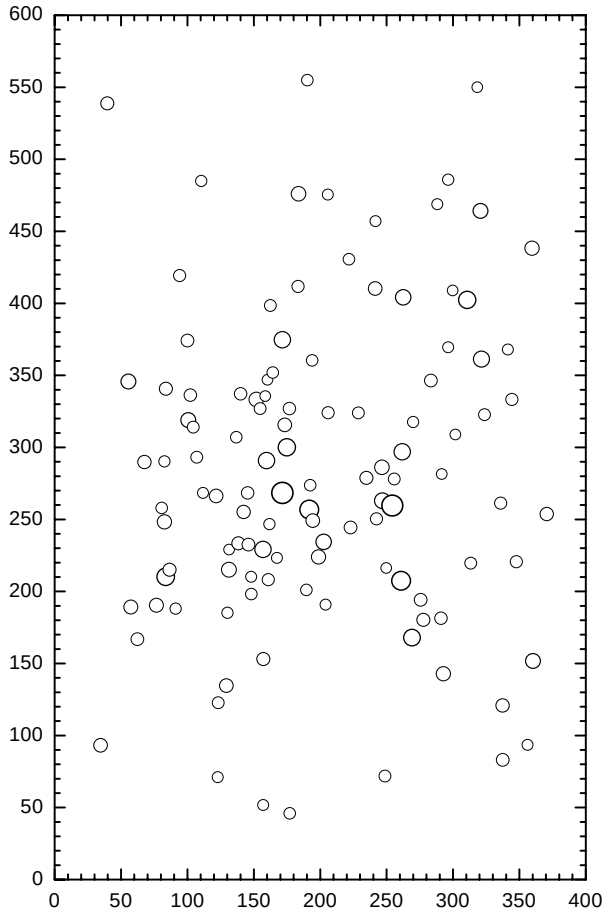

Fig. 2. Finding chart for Melotte 105. North is to the right and west is upwards; 1 pixel = 0.5″

Figure 1 shows the observed values for this cluster. Again, it is proven that the derived $(g_1 - y)$ values are suitable to derive accurate Δa-values.

Assuming that the Δa-values of the reference stars follow a normal distribution, we have calculated confidence intervals (Rees 1987) of 99.9 percent which corresponds to $3\,\sigma$ (Fig. 1).

4.2. Melotte 105

Melotte 105, a rich open cluster at a distance of 2100 pc in the fourth galactic quadrant in the vicinity of η Carinae with more than 100 stars measured (for the finding chart see Fig. 2) in our program does not exhibit any pronounced photometric peculiar star of type CP2 although it has many stars around A0 where the relative frequency of those stars reaches its maximum. Our sample shares 68 stars with the Strömgren CCD-photometry by Balona & Laney (1995) and the high degree of correlation of their $(b - y)$ values with our $(g_1 - y)$ values renders the use of the latter ones as equivalent for the purpose of deriving Δa-values. The larger negative deviations for the fainter stars of our sample (which are significantly less present in the Strömgren study) can therefore be easily ascribed to the effect of larger interstellar reddening of background stars. There are eight stars which we would call candidate λ Bootis stars: Nos. 6, 33, 38, 70, 75, 107, 112 and 113. For a review on the group of λ Bootis see Paunzen (2000).

In order to establish the line of normality for deriving the deviations Δa, we have chosen reference stars (Table 5) according to the following criteria: They had to exhibit an average behaviour in the m_1 versus $(b-y)$ and c_1 versus $(b-y)$ diagrams based on the CCD-photometric study of Balona & Laney (1995). This way 16 objects have been obtained spanning an interval in $(b - y)$ from 0.28 to 0.50 mag corresponding to a spectral type range of B9 to A8 taking the cluster reddening $E(B - V) = 0.36$ mag into account. Santos & Bica (1993) derived a reddening of $E(B - V) = 0.30$ mag and found no evidence for differential reddening throughout the cluster.

As abscissae in the a versus colour diagrams we were able to choose among three types of temperature indices: photographic $(B - V)$ values from Sher (1965), $(b - y)$ just mentioned and $(g_1 - y)$ of our own photometric system. From the poor correlation of our index with photographic $(B - V)$, we are immediately able to conclude that we should resign about using the $(B - V)$ data for deriving Δa-values. This is probable because of the rather crowded field and the uncertainties introduced by using photographic values. On the other hand it is very comforting to notice the very good correlation of CCD-based $(b-y)$ and (g_1-y). Figure 4 shows the correlation for the members of Melotte 105. Note that differential reddening would not influence this diagram since both indices are affected the same way.

Therefore we decided to derive Δa-values from normality lines based on both $(b - y)$ and $(g_1 - y)$:

$$a_0 = 0.603 + 0.139\,(b - y)$$

and

$$a_0 = 0.753 + 0.197\,(g_1 - y).$$

The Δa-values from both lines are given in Table 5 for the reference as well as program stars. They scatter around their lines by 0.0028 and 0.0034 mag, respectively.

The average scatter of the Δa-values derived from the $(b-y)$ normality line is 0.0073 mag if we regard only those 45 stars which are brighter than $V = 15$ mag. With the $(g_1 - y)$ normality line we get a scatter of 0.0079 for the 68 stars of the same brightness interval. Had we taken all objects in both cases we would have arrived at mean scatter values of 0.0088 and 0.0104 mag for $(b - y)$ and $(g_1 - y)$, respectively. The reason for the larger difference in the second case is the lower number of stars fainter than $V = 15$ mag measured by Balona & Laney (1995). Fainter stars do not only increase the scatter in Δa because of photon statistics, but also because of the higher reddening usually connected with background stars which moves

Table 5. All observed stars of Melotte 105. Objects with an asterisk denote reference stars used for the calibration process

No$_1$	No$_2$	X	Y	V	a	(g_1-y)	Δa	$(b-y)$	Δa	m_1	c_1	β
1		34.6	93.1	14.00	0.638	−0.522	−0.012					
2		39.7	538.8	14.30	0.630	−0.512	−0.022					
3*	79	55.7	345.5	13.36	0.643	−0.554	−0.002	0.280	+0.001	0.086	0.981	2.805
4	80	57.4	189.2	13.85	0.641	−0.537	−0.007	0.306	−0.005	0.102	1.068	2.846
5	81	62.4	166.8	14.40	0.638	−0.534	−0.011	0.307	−0.008	0.150	1.024	2.880
6	76	67.7	289.7	14.09	0.630	−0.526	−0.019	0.307	−0.016	0.095	1.115	
7	77	76.8	190.3	13.93	0.639	−0.534	−0.009	0.298	−0.005	0.085	1.102	
8	73	80.9	257.9	15.14	0.661	−0.407	−0.012	0.421	−0.001	0.285	0.530	
9	74	82.7	248.2	14.55	0.650	−0.539	+0.003	0.294	+0.006	0.136	0.970	
10	72	82.8	290.1	15.23	0.657	−0.455	−0.007	0.433	−0.008	0.079	1.116	
11		83.7	210.1	12.35	0.640	−0.548	−0.005					
12	71	83.9	340.7	14.32	0.641	−0.535	−0.007	0.313	−0.006	0.120	1.033	
13	49	86.6	215.0	14.35	0.657	−0.523	+0.007	0.320	+0.009	0.151	0.991	2.879
14	75	91.3	187.9	15.31	0.670	−0.459	+0.007	0.368	+0.015	0.237	0.815	
15		94.2	419.3	14.76	0.650	−0.500	−0.004					
16	66	100.1	374.0	14.47	0.641	−0.525	−0.009	0.309	−0.005	0.138	0.993	2.887
17	68	100.7	318.9	13.43	0.646	−0.511	−0.007	0.333	−0.004	0.063	1.124	2.834
18	67	102.4	336.2	14.67	0.650	−0.495	−0.006	0.357	−0.003	0.133	1.022	
19		104.5	313.9	15.00	0.657	−0.473	−0.003					
20	69	107.1	293.0	14.87	0.644	−0.493	−0.012	0.363	−0.010	0.164	0.969	
21		110.5	484.7	15.21	0.680	−0.342	−0.006					
22	45	111.8	268.4	15.64	0.654	−0.409	−0.018	0.556	−0.028	0.028	0.827	2.809
23	65	121.7	266.2	13.98	0.654	−0.550	+0.009	0.362	+0.000	0.100	1.014	
24		123.0	71.1	15.73	0.681	−0.350	−0.004					
25		123.2	122.7	14.90	0.655	−0.481	−0.004					
26		129.4	134.6	14.05	0.645	−0.526	−0.004					
27	63	130.1	185.2	15.35	0.655	−0.458	−0.008	0.430	−0.009	0.173	0.730	
28*	62	131.4	215.0	13.45	0.644	−0.548	+0.003	0.298	+0.000	0.104	1.034	2.845
29*	61	131.5	229.0	15.78	0.678	−0.413	+0.006	0.502	+0.003	0.157	0.698	2.651
30*	57	136.9	306.9	15.09	0.667	−0.439	+0.000	0.448	+0.000	0.159	0.749	2.836
31	60	138.5	233.2	14.20	0.655	−0.474	−0.005	0.426	−0.009	0.134	0.920	
32	56	140.1	337.2	14.68	0.642	−0.493	−0.014	0.356	−0.011	0.136	0.993	
33		142.4	255.0	14.17	0.630	−0.513	−0.022					
34*	52	145.4	268.3	14.63	0.657	−0.492	+0.001	0.371	+0.002	0.165	0.870	
35	53	146.1	232.5	14.34	0.646	−0.532	−0.002	0.325	−0.002	0.133	1.008	
36	54	148.1	210.1	15.69	0.682	−0.406	+0.009	0.532	+0.003	0.121	0.609	
37	55	148.2	198.0	15.01	0.659	−0.459	−0.004	0.420	−0.003	0.190	0.792	
38		151.9	333.2	13.58	0.631	−0.533	−0.017					
39*	39	154.9	326.8	14.87	0.660	−0.464	−0.002	0.408	−0.001	0.138	0.940	
40	47	156.9	229.0	12.72	0.655	−0.534	+0.007	0.320	+0.007	0.086	1.152	
41		157.2	51.7	15.43	0.678	−0.418	+0.007					
42	51	157.2	153.1	14.30	0.656	−0.531	+0.008	0.296	+0.012	0.168	0.911	2.852
43	43	158.6	335.5	15.78	0.658	−0.409	−0.015	0.451	−0.009	0.113	1.024	
44*	44	159.7	290.8	12.75	0.651	−0.541	+0.004	0.331	+0.002	0.073	1.133	
45	9	160.4	346.9	15.77	0.677	−0.438	+0.010	0.472	+0.007	0.212	0.563	
46	50	161.1	208.1	14.70	0.670	−0.499	+0.015	0.364	+0.016	0.151	0.959	2.880
47	46	161.8	246.6	15.19	0.646	−0.478	−0.013	0.436	−0.019	0.160	0.767	2.851
48		162.6	398.5	14.90	0.657	−0.499	+0.002					
49		164.3	351.9	15.10	0.636	−0.482	−0.023					
50	48	167.5	223.3	15.44	0.675	−0.496	+0.019	0.461	+0.007	0.139	0.771	2.821
51	64	171.5	268.3	11.23	0.652	−0.572	+0.012	0.272	+0.012	0.079	0.858	
52	42	171.6	374.8	12.80	0.644	−0.559	+0.001	0.310	−0.002	0.080	1.096	
53		173.4	315.6	13.96	0.638	−0.545	−0.008					
54*	40	175.0	300.0	12.45	0.646	−0.538	−0.001	0.319	−0.002	0.083	1.039	
55		176.9	326.8	14.54	0.643	−0.539	−0.004					

Table 5. continued

No_1	No_2	X	Y	V	a	(g_1-y)	Δa	$(b-y)$	Δa	m_1	c_1	β
56		177.2	45.9	15.15	0.637	−0.444	−0.029					
57		183.4	411.6	14.75	0.656	−0.509	+0.003					
58		183.8	475.9	13.53	0.628	−0.555	−0.016					
59	38	189.6	201.1	15.06	0.673	−0.467	+0.011	0.417	+0.011	0.159	0.926	2.830
60		190.5	554.8	15.06	0.657	−0.480	−0.001					
61		191.9	256.8	11.87	0.658	−0.539	+0.011					
62*	35	192.6	273.7	15.12	0.660	−0.484	+0.002	0.399	+0.000	0.156	0.888	2.861
63	33	194.1	360.2	15.07	0.641	−0.472	−0.020	0.382	−0.016	0.183	0.920	
64	36	194.5	249.1	13.98	0.654	−0.531	+0.005	0.375	−0.002	0.034	1.148	
65		198.8	223.9	13.75	0.656	−0.528	+0.007					
66		202.8	234.4	13.08	0.664	−0.531	+0.015					
67	32	204.2	190.8	15.50	0.671	−0.449	+0.006	0.437	+0.006	0.142	0.973	2.811
68		205.8	475.3	15.61	0.664	−0.411	−0.008					
69*	29	206.1	323.9	14.67	0.653	−0.501	−0.002	0.360	−0.001	0.153	0.944	
70		221.9	430.5	15.05	0.623	−0.491	−0.033					
71	26	223.0	244.3	14.43	0.650	−0.505	−0.003	0.312	+0.004	0.162	1.115	2.852
72	23	228.8	323.9	14.85	0.659	−0.481	+0.001	0.348	+0.007	0.207	0.900	
73	25	234.8	278.8	14.26	0.651	−0.524	+0.001	0.334	+0.001	0.127	1.024	2.879
74		241.5	410.2	14.04	0.633	−0.537	−0.014					
75		241.7	457.1	15.44	0.636	−0.394	−0.039					
76	20	242.4	250.4	14.74	0.675	−0.495	+0.019	0.384	+0.018	0.189	0.872	
77	19	246.6	286.1	13.52	0.657	−0.545	+0.011	0.310	+0.011	0.094	0.980	2.826
78		246.9	263.0	13.03	0.669	−0.515	+0.017					
79		248.9	71.7	14.86	0.651	−0.485	−0.007					
80	22	249.8	216.2	15.82	0.678	−0.414	+0.006	0.561	−0.005	0.215	0.475	
81		254.4	259.6	11.35	0.685	−0.388	+0.008					
82	17	255.9	277.9	14.86	0.663	−0.508	+0.010	0.364	+0.009	0.144	1.007	2.899
83	18	261.1	207.3	11.85	0.658	−0.530	+0.009	0.341	+0.007	0.075	1.197	2.808
84*	16	261.9	296.7	12.69	0.653	−0.522	+0.002	0.335	+0.003	0.091	1.131	2.810
85		262.6	404.1	13.06	0.631	−0.546	−0.015					
86	15	269.3	167.9	12.60	0.652	−0.525	+0.002	0.327	+0.003	0.084	1.029	2.804
87	12	270.2	317.5	15.23	0.655	−0.459	−0.008	0.446	−0.011	0.146	0.969	
88*	13	275.8	194.2	14.34	0.650	−0.513	−0.002	0.342	−0.001	0.127	1.108	
89*	14	277.9	180.2	14.23	0.659	−0.497	+0.003	0.371	+0.003	0.132	1.016	
90		283.3	346.3	14.48	0.654	−0.475	−0.006					
91		288.3	468.7	15.70	0.647	−0.438	−0.020					
92*	11	291.1	181.2	14.61	0.657	−0.508	+0.004	0.359	+0.003	0.128	1.059	
93	10	291.6	281.4	15.93	0.704	−0.368	+0.023	0.591	+0.016	0.050	0.716	
94		292.9	142.7	13.73	0.638	−0.536	−0.010					
95		296.4	485.8	15.30	0.647	−0.452	−0.017					
96	8	296.5	369.4	15.39	0.647	−0.458	−0.016	0.408	−0.014	0.153	0.729	
97		299.9	408.9	15.76	0.663	−0.464	+0.001					
98*	7	301.9	308.9	15.86	0.667	−0.406	−0.006	0.501	−0.007	0.199	0.682	
99		310.8	402.4	12.47	0.635	−0.544	−0.012					
100	5	313.6	219.4	14.99	0.662	−0.494	+0.006	0.370	+0.006	0.161	1.009	
101		318.3	549.9	15.84	0.660	−0.339	−0.026					
102		320.9	464.0	13.33	0.636	−0.526	−0.013					
103*	3	321.4	361.2	12.83	0.643	−0.533	−0.005	0.318	−0.004	0.077	1.056	
104	4	323.9	322.6	14.88	0.655	−0.513	+0.003	0.336	+0.005	0.169	0.864	
105	1	335.9	261.3	14.76	0.645	−0.505	−0.009	0.378	−0.012	0.136	1.055	
106		337.4	120.9	14.17	0.668	−0.378	−0.011					
107		337.6	83.0	14.37	0.625	−0.523	−0.025					
108		341.4	367.8	15.54	0.664	−0.443	−0.002					
109		344.4	333.2	14.74	0.654	−0.462	−0.008					
110		347.9	220.5	14.73	0.647	−0.512	−0.006					

Table 5. continued

No$_1$	No$_2$	X	Y	V	a	(g_1-y)	Δa	$(b-y)$	Δa	m_1	c_1	β
111		356.2	93.4	15.74	0.675	−0.429	+0.006					
112		359.6	438.2	13.74	0.633	−0.525	−0.017					
113		360.2	151.6	13.31	0.636	−0.511	−0.016					
114		370.7	253.7	14.08	0.682	−0.338	−0.005					

Column 1: Notation for stars sorted after X and Y, respectively (Fig. 2).
Column 2: Notation according to Balona & Laney (1995).
Column 3: X-coordinate in finding chart (Fig. 2).
Column 4: Y-coordinate in finding chart (Fig. 2).
Column 5: Visual magnitude from Balona & Laney (1995) or $V = -8.15 + 0.99\,y$.
Column 6: Mean a-index.
Column 7: Mean $(g_1 - y)$ value.
Column 8: Deviation from cluster line $a_0 = 0.753 + 0.197\,(g_1 - y)$.
Column 9: $(b - y)$ from Balona & Laney (1995).
Column 10: Deviation from cluster line $a_0 = 0.603 + 0.139\,(b - y)$.
Column 11: m_1 from Balona & Laney (1995).
Column 12: c_1 from Balona & Laney (1995).
Column 13: β from Balona & Laney (1995).

them away from the normality line to the right. The contrary case – foreground stars with lesser reddening – will also increase the Δa scatter, shifting the points systematically to the left, even with the possibility of mimicking a peculiar star.

Therefore the assignment of peculiarity is less straightforward in the case of clusters which are more distant than the typical clusters so far observed with conventional photoelectric Δa-photometry.

In order to check if the observed stars are really members of the cluster a colour-magnitude-diagram using $(g_1 - y)$ as temperature sensitive index and the Johnson V magnitude derived from a calibration via Strömgren y was used.

It shows that this cluster has a well defined main sequence. But the following stars are either not members of this cluster or spectroscopic binary systems: Nos. 21, 50, 51, 81, 97, 106 and 114.

From Table 5 we extract a list of four objects which may be considered as photometric CP2-candidates to be verified by spectroscopy: Nos. 46, 66, 76 and 78. But none of them could be called a substantial photometric peculiar object, since the positive deviations from the normality lines reach hardly 0.020 mag.

There seems to be quite a confusion about the age of Melotte 105 in the literature. Sher (1965) gives an age "older than NGC 3603 ($\log t = 6.0$) and younger than NGC 3496 ($\log t = 8.3$)" whereas Lyngå (1987) lists $\log t = 7.77$. Balona & Laney (1995) derive an age of $\log t = 8.4$ or 8.6 depending on the reddening used for fitting isochrones to the colour-magnitude-diagram.

4.3. NGC 6250

This young open cluster lies in a strongly obscured region at a distance of about 1000 pc. The Trümpler classification is II 3 r (for the finding chart see Fig. 5). We note that the quotation of "B8" as earliest spectral type given by Lyngå (1987) is certainly wrong. All other references (Moffat & Vogt 1975; Herbst 1977 and Fenkart & Binggeli 1979) list B1 which seems more realistic for a cluster age of about 15 million years. References for this cluster are rare in the literature. Only Moffat & Vogt (1975) presented Johnson UBV-measurements for some members, no other photometric or spectroscopic data were found.

From 13 "standard" stars (selected via their Johnson UBV-colours) we find the normality line of this cluster as:

$a_0 = 0.694 + 0.321\,(g_1 - y)$.

Table 6 lists the results. The 3σ-scatter around the normality line (0.018 mag) is higher than that derived for Melotte 105. This is probably caused by differential reddening and the presence of non-members in this field. Figure 6 shows the result graphically. The shift of the zero-point is certainly due to differential reddening. The slope of the normality line is larger than that of the other two clusters but still in the range of that found for other clusters (Maitzen 1993).

Two stars, Nos. 8 and 46, with $\Delta a = +0.026$ and $+0.065$ mag, respectively, are definite candidates for a classification as CP2. Their colours $(B-V)_0 = -0.06$ and -0.03 mag are also in agreement with the typical spectral domain of CP2 stars, if considering the mean extinction within NGC 6250 of $E(B-V) = 0.38$ mag given by Moffat & Vogt (1975) (Herbst 1977 lists $E(B-V) = 0.37$ mag). Before we are able to conclude that these two stars are positive detections, the effect of differential extinction

Table 6. All observed stars of NGC 6250. Objects with an asterisk denote reference stars used for the calibration process

No_1	No_2	X	Y	V	$(B-V)$	a	(g_1-y)	Δa
1		51.0	391.4	13.24		0.560	−0.484	+0.021
2		64.6	316.6	13.39		0.489	−0.610	−0.008
3		64.6	456.0	13.54		0.494	−0.674	+0.016
4		91.8	626.0	14.90		0.516	−0.513	−0.012
5		102.0	527.4	14.14		0.504	−0.575	−0.006
6*		142.8	724.6	11.09	0.33	0.468	−0.711	+0.003
7		200.6	687.2	14.95		0.479	−0.533	−0.045
8	28	238.0	296.2	12.43	0.35	0.492	−0.709	+0.026
9		244.8	391.4	14.81		0.513	−0.603	+0.013
10		244.8	507.0	13.88		0.540	−0.582	+0.033
11*		282.2	711.0	12.41	0.36	0.455	−0.701	−0.013
12		295.8	282.6	14.61		0.523	−0.566	+0.011
13*	27	312.8	524.0	12.48	0.75	0.522	−0.584	+0.015
14*	28	329.8	666.8	12.86	0.41	0.466	−0.697	−0.004
15		333.2	564.8	15.12		0.489	−0.575	−0.020
16		336.6	398.2	15.46		0.538	−0.481	−0.003
17*	17	340.0	758.6	10.65	0.22	0.458	−0.733	−0.003
18		408.0	333.6	15.53		0.623	−0.413	+0.061
19		408.0	534.2	15.77		0.683	−0.615	+0.186
20		544.0	299.6	14.38		0.475	−0.543	−0.045
21		547.4	561.4	14.35		0.449	−0.486	−0.089
22		554.2	537.6	14.38		0.449	−0.589	−0.056
23		581.4	595.4	14.00		0.510	−0.450	−0.039
24		581.4	748.4	14.19		0.449	−0.399	−0.117
25		591.6	452.6	14.72		0.484	−0.450	−0.065
26*		595.0	473.0	12.00	0.41	0.464	−0.688	−0.009
27*		601.8	398.2	11.10	0.19	0.471	−0.759	+0.021
28		612.0	316.6	12.57	0.40	0.438	−0.712	−0.027
29		646.0	177.2	13.71		0.485	−0.576	−0.024
30		646.0	374.4	15.51		0.556	−0.384	−0.015
31*	7	669.8	503.6	11.87	0.23	0.454	−0.742	−0.002
32		676.6	666.8	15.13		0.666	−0.129	+0.013
33*		693.6	306.4	12.73	0.63	0.500	−0.611	+0.002
34		700.4	711.0	13.87		0.479	−0.543	−0.041
35	12	714.0	299.6	12.88	0.30	0.457	−0.698	−0.013
36*		717.4	326.8	13.06	0.48	0.489	−0.673	+0.011
37*		734.4	364.2	13.59	0.49	0.468	−0.642	−0.020
38*		754.8	337.0	12.18	0.36	0.463	−0.714	−0.003
39*		771.8	388.0	12.15	0.27	0.456	−0.734	−0.002
40		778.6	136.4	13.94		0.526	−0.494	−0.009
41		785.4	88.8	12.04		0.559	−0.427	+0.003
42		846.6	82.0	15.59		0.393	−0.315	−0.199
43		853.4	697.4	14.98		0.454	−0.280	−0.150
44		894.2	119.4	13.30		0.422	−0.578	−0.087
45		935.0	340.4	12.62		0.445	−0.671	−0.033
46		952.0	241.8	12.02	0.24	0.513	−0.764	+0.065
47		989.4	364.2	13.40		0.529	−0.516	−0.003
48		1003.0	673.6	13.06		0.520	−0.387	−0.050

Column 1: Notation for stars sorted after X and Y, respectively (Fig. 5).
Column 2: Notation according to Moffat & Vogt (1975).
Column 3: X-coordinate in finding chart (Fig. 5).
Column 4: Y-coordinate in finding chart (Fig. 5).
Column 5: Visual magnitude from Moffat & Vogt (1975) or $V = -8.31 + 0.99\,y$.
Column 6: $(B-V)$ from Moffat & Vogt (1975).
Column 7: Mean a-index.
Column 8: Mean (g_1-y) value.
Column 9: Deviation from cluster line $a_0 = 0.694 + 0.321\,(g_1-y)$.

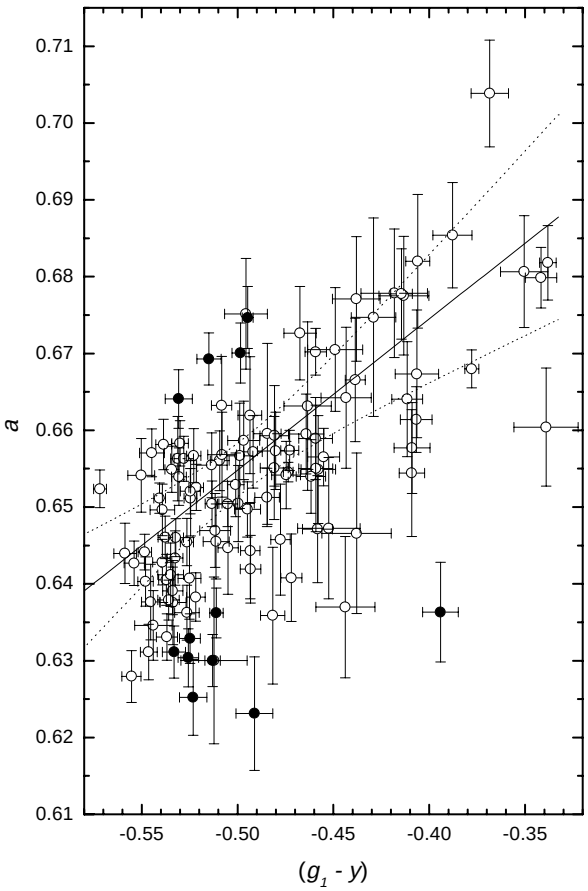

Fig. 3. a versus $(g_1 - y)$ for Melotte 105, the symbols are the same as in Fig. 1

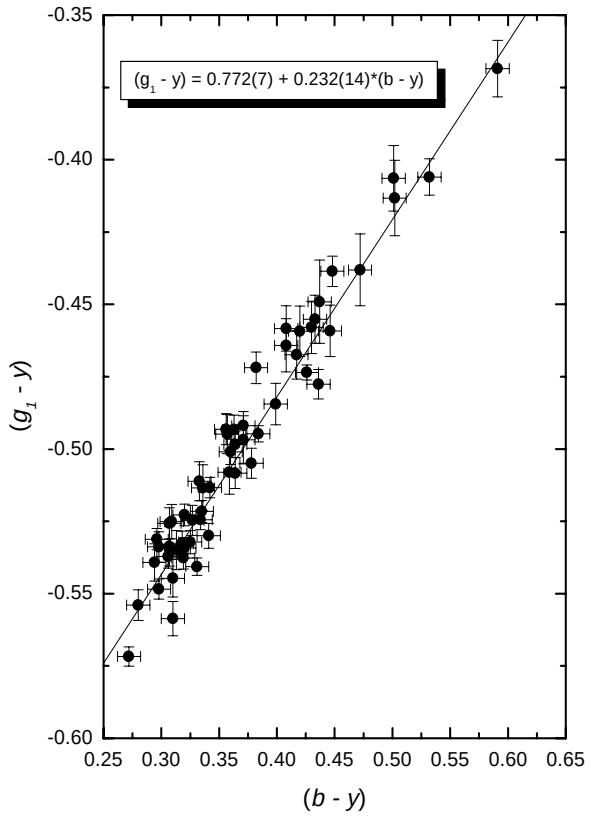

Fig. 4. $(g_1 - y)$ versus $(b - y)$ for members of Melotte 105, the values are taken from Table 5

Table 7. Stars in NGC 6250 with UBV-measurements and a spectral type of approximately A0 or earlier

No.	V	$(B-V)$	$(U-B)$	Q	$E(B-V)$
6	11.09	0.33	+0.10	−0.138	0.38
8	12.43	0.35	+0.25	−0.009	0.36
11	12.41	0.36	+0.25	−0.009	0.36
17	10.65	0.22	−0.28	−0.438	0.37
27	11.10	0.19	−0.26	−0.397	0.32
31	11.87	0.23	+0.06	−0.106	0.27
35	12.90	0.30	+0.28	−0.064	0.28
38	12.18	0.36	+0.19	−0.069	0.38
39	12.15	0.27	+0.06	−0.134	0.32
46	12.00	0.24	+0.11	−0.063	0.26

in NGC 6250 has to be investigated. The Q-method (Golay 1974) was applied to all stars with UBV-measurements, and a spectral type of approximately A0 or earlier. Table 7 lists these stars with the calculated $E(B-V)$ values.

Unfortunately, the sample of stars for which UBV-measurements are available is quite small (note that the two candidate positive CP2 detections are also included). However, if taken as representative, a mean reddening $\overline{E(B-V)} = 0.33(5)$ mag was estimated. This value is slightly less than given by Moffat & Vogt (1975) and Herbst (1977). Since our sample is not identical with those used by the other two sources, this result has to be taken with caution. Nevertheless we can state that effects of differential extinction are not negligible in NGC 6250.

The star designated as No. 19 with $\Delta a = +0.186$ mag would be one of the most extreme chemically peculiar stars ever discovered. However, this corresponds only to 1.5 times its mean error in a which is much larger than the mean errors of the other stars in the same interval of $(g_1 - y)$. Furthermore since there is strong evidence for its non-membership, this star is therefore not relevant for the current survey. Nevertheless further investigations are strongly encouraged.

Several stars with negative Δa-values cannot be regarded as peculiar for our purposes due to their large photometric errors; these are the stars Nos. 21, 22, 24, 42 and 43. Furthermore, the negative Δa-values of these objects can alternatively be explained by differential extinction. Because of these uncertainties, these stars cannot be included for statistical purposes as chemically peculiar, in contrast to the somewhat brighter stars Nos. 28 and 45. The latter two are realistic candidates for a classification as candidate λ Bootis stars, with $\Delta a = -0.027$ and $(g_1 - y) = -0.712$ mag (equivalent to a spectral type of A2), as well as $\Delta a = -0.033$ and $(g_1 - y) = -0.671$ mag

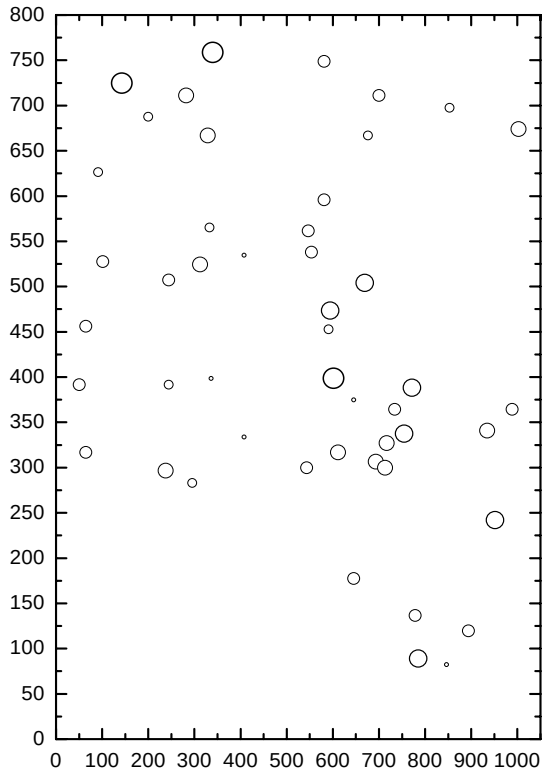

Fig. 5. Finding chart for NGC 6250. North is to the right and west is upwards; 1 pixel = 0.5″

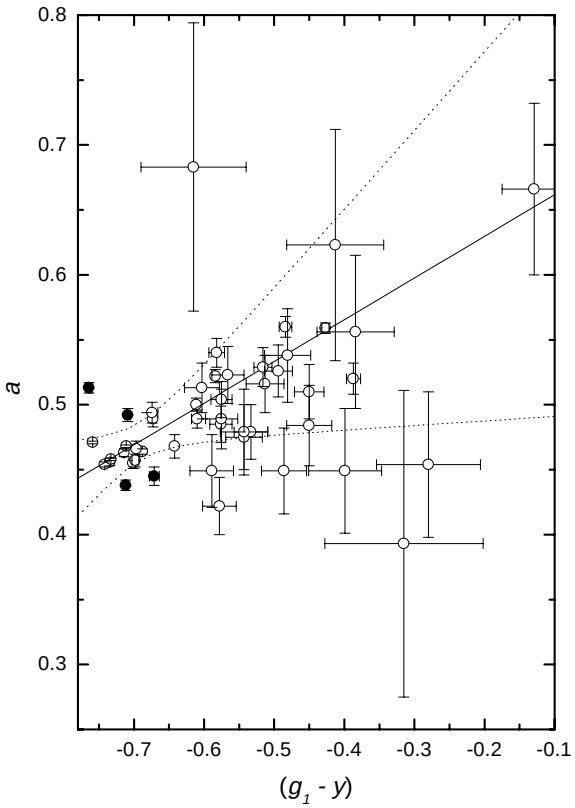

Fig. 6. a versus $(g_1 - y)$ for NGC 6250, the symbols are the same as in Fig. 1

(equivalent to of about A5), respectively. Again, further photometric and spectroscopic data are needed to decide on the true nature of these objects.

In order to check if the stars of interest are really members of the cluster a colour-magnitude-diagram using $(g_1 - y)$ as temperature sensitive index and the y colour as closely related to Johnson V was made.

The positive detections Nos. 8, 28, 45 and 46 lie well on the cluster main sequence suggesting, with a high probability, that these objects are cluster members. We are also able to conclude that the following stars are either not members of this cluster or spectroscopic binary systems: Nos. 1, 13, 19, 22, 30, 33, 41, 42, 44, 47 and 48.

5. Conclusions

We have presented Δa-photometry of 175 stars in the magnitude range $8 < V < 16$ mag for three open clusters (NGC 2169, Melotte 105 and NGC 6250). More than 100 frames in the three different colours were sampled and averaged. Aperture as well as point-spread-function-fitting photometry was applied to the crowded fields.

A comparison with previous published photoelectric measurements for NGC 2169 further proves the capability of the CCD technique together with the use of rather small telescopes (typically 60 cm) to acquire high precision photometry in order to sample the characteristic flux depression at 5200 Å.

The results for the three clusters are the following:

- NGC 2169: The known A0 Si star No. 12 was also detected with $\Delta a = +0.044$ mag (Maitzen 1993: $\Delta a = +0.042$ mag);
- Melotte 105: Four marginally peculiar CP2 as well as eight candidate λ Bootis stars were found. Beside a significant number of objects with negative Δa-values at the hotter end of the clusters main sequence, the age of this cluster needs clarification;
- NGC 6250: This cluster is affected by differential reddening. Two classical CP2 as well as two candidate λ Bootis stars were detected. It was shown that the "mosaiking-technique" does not affect the photometric accuracy.

These findings encourage us in our new survey to find chemically peculiar stars. More than two dozen open clusters in the southern as well as in the northern hemisphere were already observed and are currently reduced. As a future highlight, we have also observed two fields in the Large Magellanic Cloud in the Δa-system which means the application of this technique to an extragalactic object for the first time.

Acknowledgements. This work benefitted from the financial contributions of the City of Vienna (Hochschuljubiläumsstiftung projects: Wiener Zweikanalphotometer and H-112/95 Image Processing). EP acknowledges support from the Fonds zur Förderung der wissenschaftlichen Forschung project *S7303-AST*. We are indebted to Dr. R.O. Gray for valuable comments which helped to significantly improve this paper. Thanks are due to Profs. Dr. J. Dachs and Dr. R.J. Dettmar (Astronomisches Institut der Ruhr-Universität Bochum) as well as Dr. R.F. Garrison for the allotment of observing time at the Bochum telescope on La Silla and UTSO, Las Campanas. Further thanks go to Prof. Dr. W. Zeilinger and the staff of the workshop of the Institut für Astronomie Vienna for installing the OEFOSC instrument at the L. Figl Observatory on Mt. Schöpfl. Use was made of the Simbad, operated at CDS, Strasbourg, France.

References

Balona L.A., Laney C.D., 1995, MNRAS 277, 250
Fenkart R., Binggeli B., 1979, A&AS 35, 271
Golay M., 1974, Introduction to astronomical photometry. D. Reidel Publishing Co., Dordrecht, p. 138
Herbst W., 1977, AJ 82, 902
Hoag A.A., Johnson H.L., Iriarte B., et al., 1961, Publ. U.S. Naval Obs. 2nd Ser. 17, 349
Lyngå G., 1987, Catalogue of Open Cluster Data, 5th edition, CDS, Strasbourg
Maitzen H.M., 1976, A&A 51, 223
Maitzen H.M., 1993, A&AS 199, 1
Maitzen H.M., Hensberge H., 1981, A&A 96, 151
Maitzen H.M., Paunzen E., Rode M., 1997, A&A 327, 636
Moffat A.F.J., Vogt N., 1975, A&AS 20, 155
Paunzen E., 2000, Ph.D. Thesis, University of Vienna
Perry C.L., Lee P.D., Barnes J.V., 1978, PASP 90, 73
Preston G.W., 1974, ARA&A 12, 257
Rees D.G., 1987, Foundations of Statistics. Chapman & Hall, London, p. 244
Santos J.F.C., Bica E., 1993, MNRAS 260, 915
Sher D., 1965, MNRAS 129, 237
Vogt N., Kerschbaum F., Maitzen H.M., Faúndez-Abans M., 1998, A&AS 130, 455